

# Recession of a coal face exposed to a high temperature

JERALD A. BRITTEN

Lawrence Livermore National Laboratory, Livermore, CA 94550, U.S.A.

(Received 7 August 1985 and in final form 15 October 1985)

**Abstract**—A one-dimensional, transient model is developed to describe drying, pyrolysis, endothermic gasification and spalling (thermomechanical failure) of a wet coal face exposed to a high temperature. Such a situation occurs, for example, at the roof of an underground coal gasification (UCG) cavity. Emphasis is placed on thermochemistry, and rock mechanics are simplified by use of two parameters, a failure length and temperature, which measure the strength of the coal. Drying of the coal and convection of the evaporated water are modeled as a Stefan problem, and reaction of this water vapor with carbon at the free surface is described by an asymptotic solution in the limit of a large activation energy for this reaction. Thus, evaporation and gasification effects become analytic boundary conditions on the numerical solution to the transient heat penetration in the dry coal. Pyrolysis is treated numerically as the release of a single component in the dry coal according to one-step Arrhenius kinetics. Both surface gasification and spalling are shown to be of importance for typical UCG conditions, and their relative interaction can provide an explanation for UCG field test observations. The model, in particular the perturbation solution developed for the surface recession rate due to gasification, has applications in pyrolyzing ablative and related systems.

## INTRODUCTION

THE RECESSION of a reactive, thermally alterable, solid surface exposed to a hot environment is a phenomenon with widespread applications in the fields of chemical mechanical, aerospace and nuclear engineering, and material science. Unique among such problems is the recession of a coal face during the growth of an underground coal gasification (UCG) cavity. Perhaps the major unsolved technical problem remaining in the development of linked vertical-well UCG is the lack of adequate capability to predict the shape, size and growth rate of the UCG cavity formed by removal of the carbon *in situ*. Lateral dimensions of the cavity determine resource recovery and the optimum distance between cavities in a multi-module burn. Heat losses and undesirable water influx that occur when the cavity has grown to meet overburden rock cause a significant decline in the product gas heating value. The overall size of the cavity also influences the post-burn settling or subsidence behavior of the overburden strata. It would be highly desirable to be able to predict with some confidence the growth rate of a UCG cavity as a function of the injected gas flux and composition, and the physico-chemical properties of the coal and overburden in question. Due to the high cost, remoteness and imprecise instrumentation of full-scale UCG field tests, to this end we must rely to a large extent on the information which smaller scale experiments and appropriate mathematical modeling can give about the dynamics of cavity growth.

Several cavity growth mechanisms probably play a role at one stage or another during the evolution of a UCG cavity. One is of course direct removal of carbon at a coal-gas interface by oxygen, steam and other gasification agents. This is probably the major

mechanism during early stages of the burn. A commonly accepted view of later cavity growth envisions spalling or breaking off of relatively small chunks of dried coal from the face adjacent to the void, due to relaxation of thermomechanical and drying/pyrolysis-induced stresses at weakness planes in the coal strata. The spalled particles fall through a hot-gas-filled void space onto a char rubble bed and are removed by reaction with injected oxygen and/or steam. This view is supported in part by coring evidence from field tests [1] and by visual inspection of small scale burns [2]. During this mode of roof growth (here roof is defined as the coal-void interface) the walls, contacted by the rubble pile, can grow laterally by gasification and combustion, stress-induced rubblization, or can simply advance as an integral effect of the roof recession. Finally, purely rock-mechanical collapse of large sections of overburden caused by removal of underlying support can occur.

A general study of coal face recession during UCG entails the consideration of unsteady radiant and convective heat transfer to the coal face and conduction into the coal, producing gases by drying and pyrolysis. The possibility of these and injected gases reacting with carbon must be considered, as well as the resolution of mechanical stresses resulting from various processes, in terms of some postulated failure criteria. This general treatment presents a formidable challenge, and models to date have limited themselves to the study of largely one mechanism, or part of one mechanism, in detail. Most of these models have emphasized rock mechanics in large, multi-dimensional, finite-difference or finite-element codes (e.g. [3-5]), which treat in detail the response of a cavity wall to tensile loads and thermally induced stresses. Recently, moisture-induced stresses upon drying of the coal have been included [6].

## NOMENCLATURE

$A$	Arrhenius pre-exponential factor [Pa <sup>-1</sup> s <sup>-1</sup> ]	$W_i$	weight fraction of species $i$ in coal
$C$	heat capacity [J kg <sup>-1</sup> K <sup>-1</sup> ]	$X_c$	normalized carbon weight fraction in solid
$D_e$	effective diffusivity [m <sup>2</sup> s <sup>-1</sup> ]	$x_c$	normalized carbon weight fraction in inner reaction zone
$D_m$	binary molecular diffusivity [m <sup>-2</sup> s <sup>-1</sup> ]	$Y_w$	mole fraction of water vapor in gas phase
$e_r$	solid radiant emissivity	$y_w$	inner-zone mole fraction of water vapor
$F_g$	gas flux [mol m <sup>-2</sup> s <sup>-1</sup> ]	$z$	axial coordinate [m].
$g$	recession distance of surface due to gasification [m]		
$\dot{g}$	recession velocity of surface due to gasification [m s <sup>-1</sup> ]	Greek symbols	
$h$	convective heat transfer coefficient [W m <sup>-2</sup> K <sup>-1</sup> ]	$\alpha$	thermal diffusivity of wet coal [m <sup>2</sup> s <sup>-1</sup> ]
$K$	dimensionless group defined by equation (37)	$\delta$	activation energy perturbation parameter
$k$	thermal conductivity [W m <sup>-1</sup> K <sup>-1</sup> ]	$\varepsilon$	reaction boundary-layer thickness
$k_0$	thermal conductivity evaluated at surface [W m <sup>-1</sup> K <sup>-1</sup> ]	$\eta$	translating axial coordinate [m]
$k_i$	thermal conductivity evaluated at steam front [W m <sup>-1</sup> K <sup>-1</sup> ]	$\theta$	inner reaction zone temperature
$l$	steam front penetration length [m]	$\Lambda$	dimensionless reaction rate
$\dot{l}$	steam front velocity [m s <sup>-1</sup> ]	$\xi$	inner reaction zone stretch variable
$l_f$	failure length parameter [m]	$\rho$	density [kg m <sup>-3</sup> ]
$M_i$	molecular weight of species $i$ [kg mol <sup>-1</sup> ]	$\sigma$	Stefan–Boltzmann constant [W K <sup>-4</sup> m <sup>-2</sup> ]
$P$	pressure [Pa]	$\phi$	porosity
$Q$	dimensionless group defined by equation (33)	$\Psi$	group defined by equation (13) [s m <sup>-1</sup> ].
$q$	heat of gasification reaction [J mol <sup>-1</sup> ]	Subscripts	
$q_v$	latent heat of vaporization of water [J kg <sup>-1</sup> ]	$c$	carbon
$r$	rate of reaction [mol m <sup>-3</sup> s <sup>-1</sup> ]	$g$	gas
$T$	temperature	$p$	pyrolysis
$T_a$	activation temperature of reaction [K]	$s$	solid
$T_i$	steam front temperature [K]	$sw$	wet coal
$T_b$	heat source temperature [K]	$v$	void gas, or volatile matter
$T_r$	roof surface temperature [K]	$w$	water
$T_f$	failure temperature [K]	$0$	zeroth-order in $\delta$ expansion
$T_\infty$	ambient temperature [K]	$1$	first-order in $\delta$ expansion
$t$	time	$\infty$	ambient conditions interior to coal roof surface.
$t_{sp}$	spalling time [s]	Superscripts	
$v_r$	surface recession velocity [m s <sup>-1</sup> ]	$'$	derivative with respect to $\eta$
$v_{sp}$	spalling velocity [m s <sup>-1</sup> ]	$-$	void side of roof reaction boundary layer
		$+$	coal side of roof reaction boundary layer
		$*$	dimensional variable
		$-$	average or reference value.

These models are necessary for predicting long-term subsidence of the overburden strata after the burn, but, since they generally assume a cavity surface temperature or employ arbitrary functions for heat release in the cavity, and do not treat the possibility of reactions, they fail to model adequately the thermochemical effects which drive cavity growth in the coal seam. Chemical attack models for cavity growth, which consider reactions of carbon at the coal face have received less attention in the literature (e.g. [7, 8]), and due to the complexity of the combined heat and mass transfer processes involved, have dealt with simple

geometries. These studies generally assume that a void gas containing oxygen comes in contact with the cavity interface. However, in larger cavities containing gas with a significant concentration of combustible species, it is not difficult to envisage large regions of the coal-void interface which are removed from oxygen sources but which are actively receding by spalling and gasification. In addition, these types of models are sensitive to a parameter difficult to measure—the thickness of the ash layer which builds up at the interface due to removal of carbon from the char.

Our goal is to include effects of drying, pyrolysis,

thermomechanical failure and gasification in a simplified, one-dimensional, unsteady-state model of coal face recession. Emphasis is placed on thermochemical effects, and rock mechanics are simplified by use of two parameters which measure the strength of the coal, a failure temperature  $T_f$  and a failure (or spalling) length  $l_f$ . Although this is a highly simplified view of the spalling phenomenon, these parameters have analogs in more sophisticated rock-mechanical models. The latter parameter is related to the spacing of weakness planes in the coal, and the former can be reasonably estimated within a range.

The model developed treats the transient penetration of heat into a coal face by radiation and convection from a constant high-temperature source, considered to be the surface of a char bed reacting under quasi-steady conditions with oxygen and steam. Drying and countercurrent convection of water vapor generated at a sharp steam front between wet and dry coal is modeled analytically as a moving boundary problem. This steam can react with the char according to the stoichiometry  $H_2O + C \rightarrow CO + H_2$ . This is a highly activated and highly endothermic reaction. As such, it is recognized that this reaction will typically be confined to a narrow boundary layer at the coal-void interface which can be considered as a front analogous to the steam front. Therefore, leading-order effects of this reaction can be analyzed by a technique known as activation energy asymptotics. This theory has in recent years been increasingly applied by many investigators to describe analytically or to simplify the numerical treatment of complex phenomena that

occur in gas-phase combustion (e.g. [9–12]), and in heterogeneous gas–solid combustion and combustion in porous media (e.g. [13, 14]). It exploits the large activation temperature characteristic of combustion processes to develop and solve the governing equations by asymptotic expansions in terms of an activation temperature perturbation parameter. A monograph by Buckmaster and Ludford [15] is devoted to this subject. Here, it is applied to a strongly endothermic heterogeneous reaction, assumed to be described by single-step, first-order Arrhenius kinetics, to provide an excellent approximation to the time-dependent surface recession due to gasification, without solving the transient species balance equations numerically. This approach for treating the surface reaction can also be used to describe possible surface reactions in pyrolyzing ablative systems (discussed by Laub *et al.* [16]).

Spalling is simulated by redefining the coal–void interface when the temperature at a distance  $l_f$  into the dry coal exceeds  $T_f$ . In the following sections the equations for thermal penetration and surface reaction are derived, the numerical solution is briefly discussed, and salient results of the model are presented. The derivation does not include effects of pyrolysis, which are developed and discussed in a later section.

## MODEL FORMULATION

We assume that oxygen injected into the bottom of the coal seam reacts with the spalled char rubble and is completely consumed in the char bed. This conceptualization is shown in Fig. 1. It implies that spalling

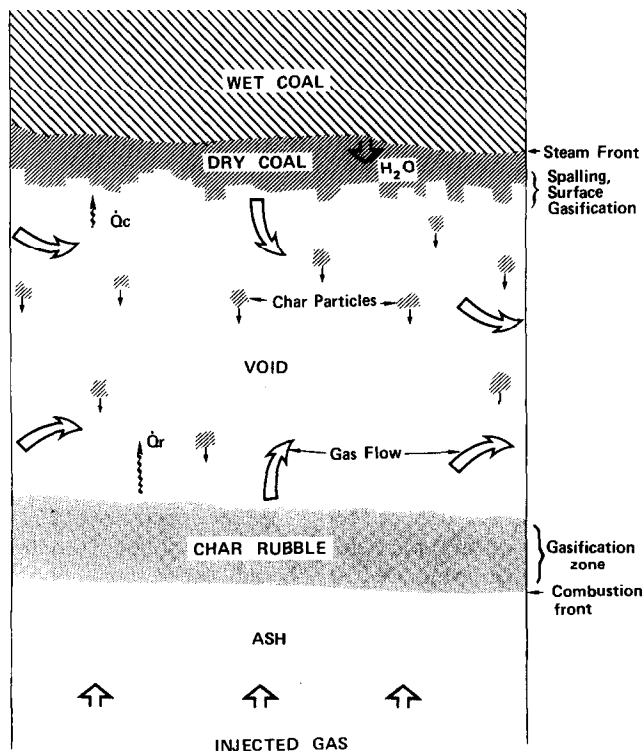


FIG. 1. Mode of cavity growth considered by model.

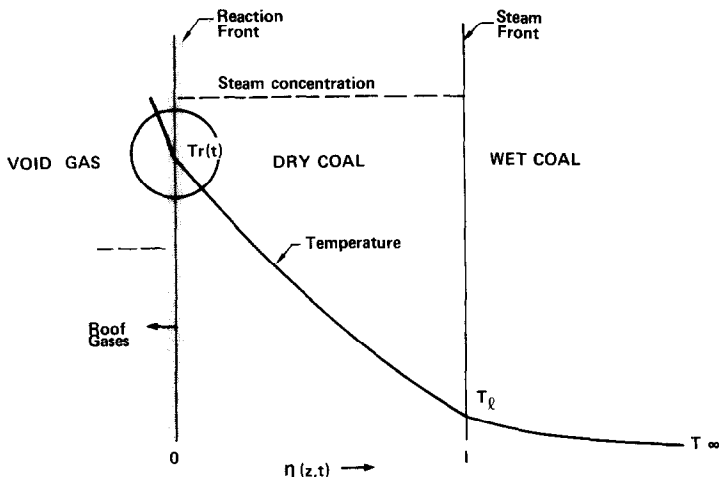


FIG. 2a. Schematic of idealized heated coal roof, showing drying and gasification fronts, temperature and steam flux profiles.

of the roof coal is an important growth mechanism at the coal-void interface. As such, the model describes the intermediate and later stages of UCG cavity growth, after it has grown by chemical attack to dimensions sufficiently large to permit spalling to occur. For reasonably thick coal seams, this mode of operation can describe the major period of gas production during a UCG operation.

Radiation from the surface of this reacting char bed—assumed to be at a constant temperature—and convective heating from the void gas, supply heat to the coal face. A side-view schematic of the idealized roof dynamics is shown in Fig. 2. Water saturating the solid evaporates at a sharp steam front of temperature  $T_l$  located at a distance  $l(t)$  measured from the original position of the free surface at time  $t = 0$ . We do not solve the momentum equation in the dry coal region, but instead demand no accumulation in the gas phase, such that all steam generated percolates out in the  $-z$ -direction, at a rate proportional to  $\dot{l} = dl/dt$  determined by an energy balance at this front. Permeation of water through the wet coal is not considered, although it can be easily included. The steam generated will react with the carbon in the dry coal initially at the free surface if the temperature is sufficiently high. The strongly endothermic reaction will absorb heat at the surface and reduce the heat flux into the interior of the coal, keeping the interior below the temperature necessary for this reaction to be significant. Therefore, unless conditions are such that complete reaction of the exiting steam is attained, the reaction will be confined to a thin zone at the free surface which can be modeled as a front, as previously discussed. Its cumulative effect can be described by a length  $g(t)$  which measures the distance of the free surface from its original position at  $t = 0$ , such that  $\dot{g} = dg/dt$  is the instantaneous free surface velocity and is a measure of the gasification rate. If complete consumption of the steam occurs, the reaction zone will continue to be very thin, but will

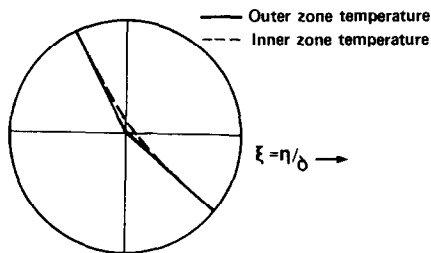


FIG. 2b. Magnification of reaction front at roof surface, showing inner reaction zone temperature (dashed line) matched with outer zone temperatures (solid lines).

detach from the surface and penetrate into the dry coal. In this event, the additional possibility of steam and  $\text{CO}_2$  diffusion from the void gas to the surface and its subsequent reaction must also be considered. This case can be important on vertical surfaces in which gravity does not facilitate spalling and the associated surface renewal. We are interested in spalling mechanisms here, however, and limit ourselves to the case where the reaction is thermally limited, and not limited by reactant supply. Such is typically the case for UCG conditions. Kinetic constants for the steam char reaction from Gibson and Euker [17] are used, and are given, along with other parameter values used in the calculations, in Table 1.

The situation shown in Fig. 2 will continue to evolve until a spall occurs. Then the spalled particle falls into the rubble bed, exposing fresh coal to be heated and spalled in an analogous manner. The existence of cracks penetrating into the dried coal is simplified by this conceptualization. These cracks can act to a certain extent to distribute the steam flow nonuniformly in the dry coal, but crack formation and propagation in this system is a poorly understood phenomenon, and modeling it would require the inclusion of one or

Table 1. Parameter values used in calculations

Wet coal density and composition	
$\rho_s = 1360 \text{ kg m}^{-3}$	
$W_c = 0.4, W_w = 0.2, W_v = 0.3, W_a = 0.1$	
Kinetic constants	
$A = 4.13 \times 10^{-3} \text{ Pa}^{-1} \text{ s}^{-1}, T_a = 17500 \text{ K}$	
Heat capacities	
$C_{gp} = 42 \text{ J mol}^{-1} \text{ K}^{-1}$	
$C_{sw} = 2100, C_s = 1650, C_w = 2055 \text{ J kg}^{-1} \text{ K}^{-1}$	
Heat effects	
$q = 136 \text{ kJ mol}^{-1}, q_v = 2170 \text{ kJ kg}^{-1}$	
Temperatures	
$T_i = 373 \text{ K}, T_\infty = 290 \text{ K}$	
Miscellaneous	
$P = 1.05 \text{ MPa}, h = 50 \text{ W m}^{-2} \text{ K}^{-1}, e_r = 0.95, \sigma = 5.6762 \times 10^{-8} \text{ W m}^{-2} \text{ K}^{-4}$	
$k_{sw} = 0.35 \text{ W m}^{-1} \text{ K}^{-1}, \rho_w = 990 \text{ kg m}^{-3}, M_{gp} = 18 \text{ g mol}^{-1}$	

more arbitrary parameters. Thus, it is not considered explicitly in the model.

Interior to the coal-void interface, gas and solid phases are assumed in local thermal equilibrium. The void gas temperature is assumed to be the arithmetic average of the heat source and instantaneous roof surface temperatures. Constant average specific heats for the dry and wet coal and steam have been assumed. The thermal conductivity of the dry coal, however, is allowed to vary with temperature according to a polynomial fit of the data given by Badzioch *et al.* [18]:

$$k = -0.15 + 3.03 \times 10^{-3} T - 6.54 \times 10^{-6} T^2 + 4.51 \times 10^{-9} T^3, \quad 300 < T < 1200 \text{ K.} \quad (1)$$

which, due to the nature of its temperature dependence, is presumed to account for a significant radiative component at high temperatures.

The wet coal has a density  $\rho_s$  and a composition, by weight percent, of  $W_w, W_c, W_v$ , and  $W_a$ , where the subscripts denote water, carbon, volatile matter and ash, respectively. The water is assumed to fill the available void space of the coal, such that the porosity of the dry coal is given by:

$$\phi = \frac{W_w \rho_s}{\rho_w}. \quad (2)$$

In stationary  $(z, t)$ -coordinates, where dimensional variables are denoted by \*, the energy balance in the wet coal is:

$$\frac{\partial T^*}{\partial t^*} = \alpha \frac{\partial^2 T^*}{\partial z^{*2}} \quad (3)$$

where  $\alpha = k_{sw}/\rho_s C_{sw}$  is the (constant) thermal diffusivity in this region. This equation is subject to the boundary conditions:

$$T^*(l, t^*) = T_i, \quad T^*(\infty, t^*) = T^*(z^*, 0) = T_\infty. \quad (3a)$$

In the dry zone, the energy, carbon and steam balances and their associated boundary and initial condition are:

$$(1 - W_w) C_s \frac{\partial(\rho_s T^*)}{\partial t^*} + C_w \frac{\partial(F_s T^*)}{\partial z^*} = \frac{\partial}{\partial z^*} \left( k \frac{\partial T^*}{\partial z^*} \right) - q r^* \quad (4)$$

$$T^*(z^*, 0) = T_\infty, \quad T^*(l, t^*) = T_i \quad (4a)$$

$$-k \frac{\partial T^*}{\partial z^*} \Big|_{\text{surface}} = \frac{\sigma e_r}{2 - e_r} (T_s^4 - T_r^4) + h(T_v - T_r)$$

$$\frac{\partial \rho_c^*}{\partial t^*} = -M_c r^* \quad (5)$$

$$\rho_c^*(0) = \rho_s W_c \quad (5a)$$

$$\frac{d(F_s Y_w)}{dz^*} = \frac{d}{dz^*} \left( \rho_s D_o \frac{dY_w}{dz^*} \right) - r^* \quad (6)$$

$$Y_w(l) = 1. \quad (6a)$$

The usual quasi-steady approximation for the gas phase has been employed in writing the above equations, thus rendering (6) an ordinary differential equation. The steam/char reaction rate is assumed to be described by:

$$r^* = \frac{A \rho_c^* P Y_w e^{-T_v/T^*}}{M_c}. \quad (7)$$

An energy balance at the steam front  $z^* = l(t)$  determines the steam flux:

$$\rho_s W_w q_v \dot{l} = -M_w q_v F_s = -k_i \frac{\partial T^*}{\partial z^*} \Big|_{l^-} + k_{sw} \frac{\partial T^*}{\partial z^*} \Big|_{l^+}. \quad (8)$$

The problem is simplified by introducing a moving coordinate system attached to the free surface and normalized over the dry zone length:

$$\eta = \frac{z^* - g(t^*)}{l(t^*) - g(t^*)}. \quad (9)$$

The derivatives transform as follows:

$$\frac{\partial}{\partial z^*} = \frac{1}{l-g} \frac{\partial}{\partial \eta}, \quad \frac{\partial^2}{\partial z^{*2}} = \frac{1}{(l-g)^2} \frac{\partial^2}{\partial \eta^2} \quad (9a)$$

$$\frac{\partial}{\partial t^*} \Big|_z = \frac{\partial}{\partial t^*} \Big|_\eta - \frac{\dot{g} + \eta(\dot{l} - \dot{g})}{l-g} \frac{\partial}{\partial \eta}.$$

Scale factors for temperature and carbon concentration are:

$$T = T^*/T_i, \quad X_c = \frac{\rho_c^*}{W_c \rho_s}. \quad (10)$$

We have chosen not to scale the time, since it is the running variable in the simulation. Thus, it will continue to be written with a \* superscript.

The wet zone energy balance and its boundary and

initial conditions, written in the  $\eta$ -coordinate system, become:

$$\frac{\partial T}{\partial t^*} = \frac{\dot{g} + \eta(\dot{l} - \dot{g})}{l - g} \frac{\partial T}{\partial \eta} + \frac{\alpha}{(l - g)^2} \frac{\partial^2 T}{\partial \eta^2} \quad (11)$$

$$T(1, t^*) = 1$$

$$T(\infty, t^*) = T(\eta, 0) = T_\infty/T_l \quad (11a)$$

This equation and its boundary and initial conditions meet the requirements of a self-similar function, independent of time in the  $\eta$ -coordinate system [19]. Accordingly, the time derivative term is dropped from (11) and the resulting equation is solved to obtain the temperature profile in the wet coal:

$$T = T_\infty/T_l + \frac{(T_l - T_\infty)\{\text{erf}[\Psi(g + (\dot{l} - \dot{g})\eta)] - 1\}}{T_l\{\text{erf}[\Psi\dot{l}] - 1\}} \quad (12)$$

where

$$\Psi = \sqrt{(l - g)/[2\alpha(\dot{l} - \dot{g})]} \quad (13)$$

This formulation (insofar as the assumption of constant wet-coal properties) is valid for general free-surface boundary conditions, and resolves the difficulty of tracking the steam front motion when the equations are solved numerically in both wet and dry zones [6, 20].

In keeping with our assumption concerning the existence of a reaction boundary layer, we define an outer zone in the dry coal and discard the reaction term in this zone as being exponentially small in the limit of a very large activation temperature. Accordingly, we define  $\delta = T_l/T_a \ll 1$  as the perturbation parameter and write the dependent variables as power series expansions of a function  $\varepsilon(\delta)$  to be determined in the inner-zone analysis:

$$\begin{aligned} T &= T_0 + \varepsilon(\delta)T_1 + o(\delta) \\ Y_w &= Y_{w0} + \varepsilon(\delta)Y_{w1} + o(\delta) \\ X_c &= X_{c0} + \varepsilon(\delta)X_{c1} + o(\delta) \end{aligned} \quad (14)$$

We are interested only in the leading-order solution to this problem, and subsequently drop the subscript 0 from the dependent variables except where needed. It should be remembered, however, that we are solving for the first term of an asymptotic expansion to the reaction-zone problem. In the outer zone, the transformed balance equations and their boundary and initial conditions become:

$$\begin{aligned} \frac{\partial T}{\partial t^*} &= \left[ \frac{\dot{g} + \eta(\dot{l} - \dot{g})}{l - g} + \frac{W_w C_w \dot{l}}{(1 - W_w)C_s(l - g)} \right] \frac{\partial T}{\partial \eta} \\ &+ \frac{1}{(1 - W_w)\rho_s C_s(l - g)^2} \frac{\partial}{\partial \eta} \left( k \frac{\partial T}{\partial \eta} \right) \end{aligned} \quad (15)$$

$$T(\eta, 0) = T_\infty/T_l, \quad T(1, t^*) = 1 \quad (15a)$$

$$\frac{\partial X_c}{\partial t^*} = \frac{\dot{g} + \eta(\dot{l} - \dot{g})}{l - g} \frac{\partial X_c}{\partial \eta} \quad (16)$$

$$X_c(\eta, 0) = X_c(1, t^*) = 1. \quad (16a)$$

$$\frac{dY_w}{d\eta} = \frac{M_w \bar{\rho}_g \bar{D}_c}{\rho_s W_w (l - g)} \frac{d}{d\eta} \left( \rho_g D_c \frac{dY_w}{d\eta} \right) \quad (17)$$

$$Y_w(1) = 1, \quad \left. \frac{dY_w}{d\eta} \right|_{1-} = 0. \quad (17a)$$

Discarding the dispersion term in the steam balance equation greatly simplifies the analysis of the inner reaction zone. In order to provide some justification for this, the coefficient multiplying this term in equation (17) must be small compared with unity, where  $\bar{D}_c$  and  $\bar{\rho}_g$  are, respectively, values for the effective molecular diffusivity and gas density evaluated at a characteristic reaction temperature. We will assume this group is small and proceed, and later check this assumption with the calculated values and an estimate of  $\bar{D}_c$ .

In this outer zone, the carbon and steam balance equations admit the trivial solutions:

$$X_c = Y_w = 1. \quad (18)$$

and the solution to (15) is to be determined numerically with the aid of two equations to be derived from an analysis of the inner reaction zone; one for the temperature derivative at  $\eta = 0^+$ , and one for the gasification velocity  $\dot{g}$ , both expressed in terms of the surface temperature  $T_l(t)$ .

An implicit equation for the steam front velocity  $\dot{l}$  in the transformed coordinate system is obtained from (8) and (12):

$$\begin{aligned} \dot{l} &= \frac{T_l}{(l - g)\rho_s q_v W_w} \\ &\times \left\{ \frac{2k_{sw}(T_l - T_\infty)\Psi(\dot{l} - \dot{g})}{\sqrt{\pi T_l}(\text{erf}[\Psi\dot{l}] - 1)} e^{-\Psi^2 \dot{l}^2} - k_l \left. \frac{\partial T}{\partial \eta} \right|_{1-} \right\}. \end{aligned} \quad (19)$$

## ANALYSIS OF REACTION ZONE

Across the inner zone, as shown in Fig. 2, we expect the temperature to be continuous but have a discontinuous first derivative, while the steam and carbon concentrations go through an  $O(1)$  change, the latter from 1 to 0. Accordingly, a stretched length coordinate is introduced to scale the dependent variable variations properly:

$$\xi = \eta/\varepsilon \quad (20)$$

and the dependent variables are expanded in  $\varepsilon$  as functions of  $\xi$ :

$$\begin{aligned} T &= T_{r0}(t^*) + \varepsilon\theta_1(\xi, t^*) + o(\delta) \\ X_c &= x_{c0}(\xi, t^*) + \varepsilon x_{c1}(\xi, t^*) + o(\delta) \\ Y_w &= y_{w0}(\xi, t^*) + \varepsilon y_{w1}(\xi, t^*) + o(\delta) \end{aligned} \quad (21)$$

When these expansions and  $\xi$  are introduced into the general energy balance [given by (15) with the inclusion of the reaction term] analysis of the argument of the exponent in the reaction term shows:

$$\exp \left[ \frac{-1}{\delta(T_{r0} + \varepsilon\theta_1 + \dots)} \right] \approx e^{-1/\delta T_{r0}} e^{\varepsilon\theta_1/\delta T_{r0}^2}. \quad (22)$$

This gives a definition for the boundary layer thickness  $\varepsilon$ :

$$\varepsilon = \delta T_{r0}^2. \quad (23)$$

By discarding terms in the inner-zone energy balance multiplied by nonzero powers of  $\varepsilon$ , we obtain the leading-order form of this equation:

$$\frac{T_1 k_0}{(l-g)^2} \frac{d^2 \theta_1}{d\xi^2} = \frac{\varepsilon q A W_c \rho_s P e^{-1/\delta T_{r0}}}{M_c} x_{c0} y_{w0} e^{\theta_1}. \quad (24)$$

Note that the reaction rate term is retained although it is multiplied by  $\varepsilon$ . This is necessary for a nontrivial solution, and implies that the coefficient of the reaction term is  $O(1/\varepsilon)$ . Note also that convective and time-dependent terms are of higher order, and  $k$  is not a function of  $\xi$  to leading order.

In a similar fashion, the leading-order balance equations for carbon and steam are obtained:

$$\frac{\rho_s W_c \dot{g}}{(l-g)M_c} \frac{dx_{c0}}{d\xi} = \frac{\varepsilon A \rho_s W_c P e^{-1/\delta T_{r0}}}{M_c} x_{c0} y_{w0} e^{\theta_1} \quad (25)$$

$$\frac{\rho_s W_w \dot{g}}{M_w(l-g)} \frac{dy_{w0}}{d\xi} = \frac{\varepsilon A \rho_s W_c P e^{-1/\delta T_{r0}}}{M_c} x_{c0} y_{w0} e^{\theta_1}. \quad (26)$$

Rigorously, since two moles of gas are generated by reaction of one mole of steam, and the solid density changes across the front, the inner-zone forms of the continuity equations for the two phases should be included in the analysis. These were included in a similar analysis of reverse gas-solid combustion in a combustible porous medium [21] and it was found that, while adding considerably to the algebraic complexity, the quantitative effect on the solution was insignificant. We therefore use the values of the gas flux and solid density on the solid (+) side of the reaction front, and hold them constant.

Matching the inner expansions with the outer expansions to leading order results in [11, 12, 15]:

$$\lim_{\xi \rightarrow \pm\infty} T_{r0} = T_0^\pm, \quad x_{c0} = X_{c0}^\pm, \quad y_{w0} = Y_{w0}^\pm \quad (27)$$

$$\theta_1 = T_0^\pm \xi + T_1^\pm$$

where the superscripts + and - denote the value on the interior and void side of the dry coal surface, respectively, and ' denotes differentiation with respect to  $\eta$ . Following the analysis of Peters [11], we conclude that  $T_1^- = T_1^+ = 0$ , that is, no higher-order perturbations are introduced by the reaction zone into the outer-zone solutions. The above outer-zone boundary conditions are given by:

$$\eta = 0^-$$

$$-T'' = \frac{(l-g)}{k_0 T_1} \left\{ \frac{\sigma e_r}{2-e_r} [T_b^4 - (T_{r0} T_1)^4] + h(T_v - T_{r0} T_1) \right\}$$

$$X_c = 0, \quad Y_w = Y_w^-. \quad (28)$$

$$\eta = 0^+$$

$$T' = T'^+, \quad X_c = 1, \quad Y_w = 1. \quad (29)$$

Note that the asymptotic behavior of  $\theta_1$  on either side of the reaction zone is

$$\lim_{\xi \rightarrow \pm\infty} \theta_1 \rightarrow \mp\infty.$$

The unknowns in this system are  $Y_w^-$ ,  $\dot{g}$  and  $T_{r0}$ , since  $T'^+$  can be obtained from the numerical solution of the outer zone energy balance if  $T_{r0}$  is known.

To solve this system, we first combine (25) and (26) and integrate, using boundary conditions at  $\eta = 0^+$ :

$$y_{w0} = 1 + \frac{W_c M_w \dot{g}}{M_c W_w l} (x_{c0} - 1). \quad (30)$$

Evaluation of (30) at  $\lim_{\xi \rightarrow -\infty}$  gives  $Y_w^-$  in terms of  $\dot{g}$ :

$$Y_w^- = 1 - \frac{W_c M_w \dot{g}}{M_c W_w l}. \quad (31)$$

Analogously, we combine (24) and (25) and solve, using boundary conditions at  $\eta = 0^-$ :

$$x_{c0} = \frac{1}{Q} \left( \frac{d\theta_1}{d\xi} - T'^- \right). \quad (32)$$

where

$$Q = \frac{q(l-g)\rho_s W_c \dot{g}}{T_1 k_0 M_c}. \quad (33)$$

Evaluation of (32) at  $\lim_{\xi \rightarrow +\infty}$  gives one of the relations needed between  $\dot{g}$  and the jump in the temperature derivative across the front:

$$T'^+ - T'^- = Q. \quad (34)$$

Equations (30) and (32) can be used in (24), to develop an equation involving only  $\theta_1$  and its derivatives:

$$\frac{d^2 \theta_1}{d\xi^2} = \Lambda \left( \frac{d\theta_1}{d\xi} - T'^- \right) \left( \frac{d\theta_1}{d\xi} + K - T'^- \right) e^{\theta_1}. \quad (35)$$

where,

$$\Lambda = \frac{T_1 k_0 M_w \varepsilon A P e^{-1/\delta T_{r0}}}{q \rho_s W_w l \dot{g}}. \quad (36)$$

and:

$$K = \frac{q(l-g)\rho_s W_w \dot{g}}{T_1 k_0 M_w} \left( 1 - \frac{W_c M_w \dot{g}}{W_w M_c l} \right). \quad (37)$$

Interestingly, (35) can be integrated analytically once, but the solution cannot give an expression for the eigenvalue  $\Lambda$  since it diverges at  $\lim_{\xi \rightarrow -\infty}$ . A local analysis of (35) near this boundary shows:

$$\lim_{\xi \rightarrow -\infty} \theta_1 \approx T'^- \xi - \frac{K e^{-T'^- \xi}}{T'^- \xi} \left( 1 - \frac{1}{T'^- \xi} + \dots \right), \quad (38)$$

which gives an indication of the rapidity of decay of

the inner solution to its value given by the outer-zone boundary condition.

Our goal is to develop an algebraic solution for the gasification front velocity in terms of the temperature and its derivative at the free surface. This must be done by analyzing the results of a numerical solution of (35). This equation contains three parameters. To reduce the parametric dependence for ease of interpretation, we use the arithmetic average of the steam concentration on both sides of the reaction front, given by the imposed boundary condition at  $\eta = 0^+$  and by equation (31):

$$\langle y_{w0} \rangle = 1 - \frac{W_c M_w \dot{g}}{2 M_c W_w l} \tag{39}$$

to give from (35):

$$\frac{d^2 \theta_1}{d\xi^2} = \bar{\Lambda} \left( \frac{d\theta_1}{d\xi} - T'^- \right) e^{\theta_1} \tag{40}$$

where:

$$\bar{\Lambda} = \frac{\varepsilon AP(l-g)}{\dot{g}} \left( 1 - \frac{W_c M_w \dot{g}}{2 W_w M_c l} \right) e^{-1/\delta T_{r0}} \tag{41}$$

Joulin and Mitani [22] have shown for premixed gas-phase combustion problems that the effect of the abundant component on the reaction-zone dynamics is only important near the stoichiometric limit. Therefore approximations such as the above are considered reasonable as long as  $O(1)$  amounts of the abundant reactant (steam in this case) exit the reaction zone.

Equation (40) was solved numerically by choosing values for  $T'^+$ ,  $T'^-$  and  $T_r$ , starting the solution at large positive values of  $\xi$  and iterating on  $\bar{\Lambda}$  until the correct boundary condition for large negative values of  $\xi$ , given by (30), was attained. It was discovered that curves of  $\bar{\Lambda}/T'^-$  vs  $(T'^+ - T'^-)/T'^-$  are identical, independent of the magnitude of  $T'^+$  or  $T'^-$ . Thus, the solution for  $\bar{\Lambda}$

can be represented by:

$$-\bar{\Lambda}/T'^- \approx 0.56(T'^+/T'^-)^{1.45} \tag{42}$$

The close agreement between this function and the numerical solution of (40) is shown in Fig. 3. Equations (34) and (42) now provide sufficient information to describe the surface gasification dynamics.

**NUMERICAL TREATMENT**

Equation (15) is solved numerically by the method of lines [23] by dividing the dry coal zone  $0 \leq \eta \leq 1$  into equally spaced increments and discretizing the spatial temperature derivatives at the nodal points. An initial temperature profile is imposed on the  $\eta$ -space, and the resulting set of ordinary differential equations in time is solved as an initial value problem, using a versatile stiff integration package LSODE developed by Hindmarsh [24]. The boundary conditions for the steam front velocity, gasification front velocity and surface temperature, represented by equations (19), (34) and (42) are solved simultaneously by Newton-Raphson iteration. Due to the exponential temperature dependence of the reaction rate,  $\dot{g}$  increases several orders of magnitude as the free surface heats up. However, since the stiffness occurs in the boundary conditions, there is no stability problem associated with use of centered differences for the convective term of the spatial discretization, as is the case when such reaction terms are included directly in the numerical solution in the bulk phase (e.g. [25]).

During the course of the solution, when the temperature at  $l_r$  exceeds  $T_r$ , the dry-zone length  $l$  is redefined as the difference between  $l(t^*)$  and  $l_r$ ,  $\dot{g}$  is set to zero, nodal points are re-zoned and the temperature at the nodes is determined by interpolation between the

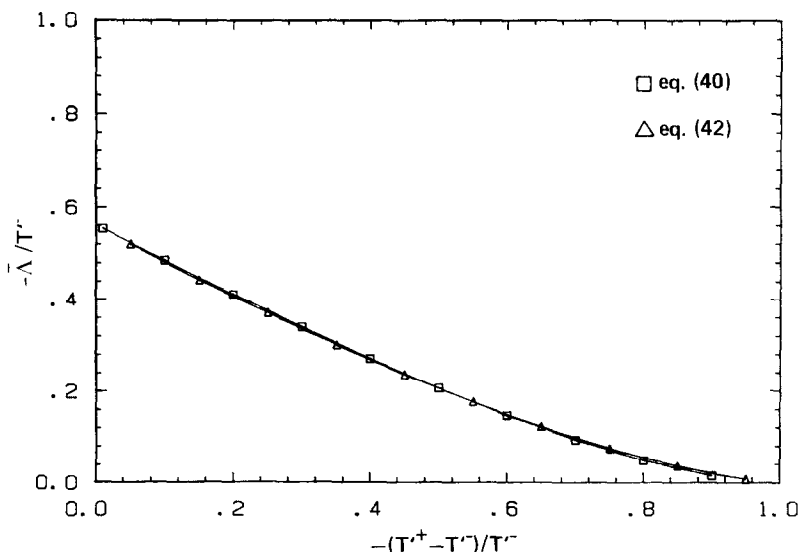


FIG. 3. Comparison of numerical solution of equation (40) and curve fit given by equation (42).



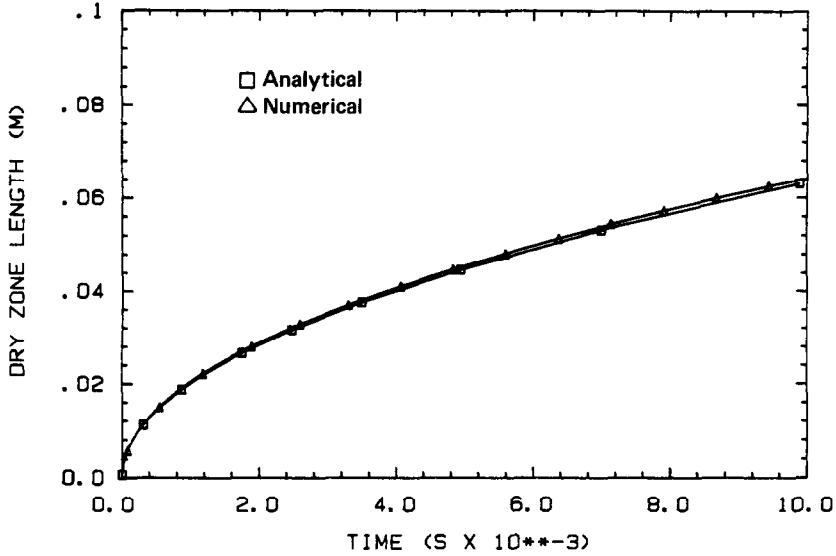


FIG. 4. Comparison of numerical prediction of steam front location for case of drying only, with analytical solution for identical conditions.  $T_r = 1100$  K,  $k_r = 0.45$  W m<sup>-1</sup> K<sup>-1</sup>. See Table 1 for other property values.

old values. The calculation is repeated until the time between spalls remains relatively constant.

**RESULTS AND DISCUSSION**

The accuracy of the numerical solution for the problem of drying only was tested by comparing numerical calculations for  $l(t)$  with those of an analytical solution to this problem obtained for the case of constant property and surface temperature values [26, 27]. The comparison used 15 internal nodes for the numerics. The satisfactory agreement between the two solutions is shown in Fig. 4.

The nature of the solution for the gasification front velocity was investigated by assuming a large excess of steam, fixing the heat source temperature at 1200 K, and calculating  $\dot{g}$  as a function of  $T_r$  via equation (42). The results of this exercise are shown in Fig. 5. Note that multiple solutions for the surface velocity exist for a range of  $T_r$ . The uppermost curve of Fig. 5 represents a hypothetical solution, independent of kinetics, which corresponds to the surface heat flux being entirely absorbed by the gasification reaction leaving none to be conducted into the coal. Since this conduction supplies one reactant in the real system, this solution will not be observed. The lower curve exhibits a turning point

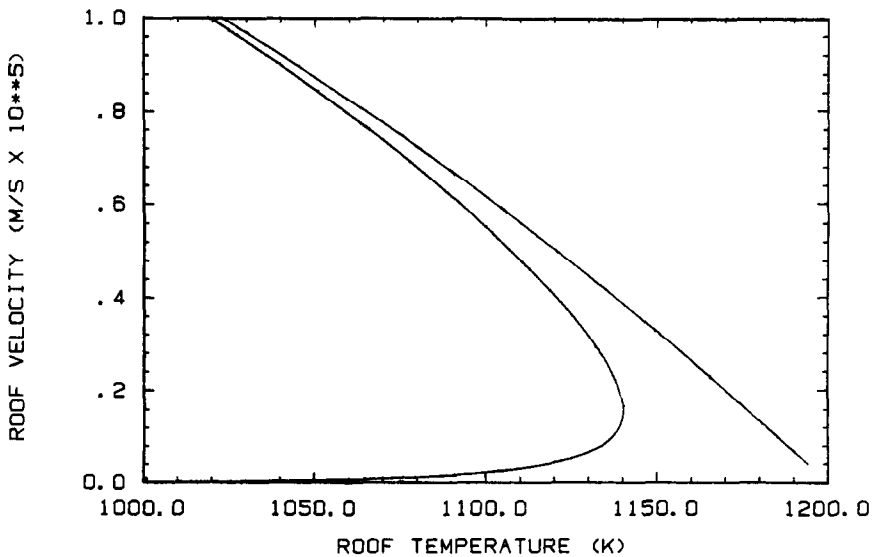


FIG. 5. Roof gasification velocity  $\dot{g}$  vs surface temperature  $T_r$  from solution of equation (42). Large excess of steam and heat source temperature of 1200 K assumed. Note ignition behavior. Uppermost curve is heat transfer limited solution.

which corresponds to an 'ignition' point for an exothermic reaction, but which cannot be attained for this endothermic reaction. The physics of the real system will conspire to keep the solution on the lower branch of the lower curve, until complete reaction of the steam occurs.

Solutions for drying only, and drying plus gasification were compared under otherwise identical conditions. Figure 6 compares surface temperatures as functions of time. Both cases show a rapid increase in surface temperature initially, followed by an extended period in which it remains relatively constant. The surface on which gasification occurs levels off at about 30 K lower than the other. This may not appear to be significant at temperatures of greater than 1100 K, but since the heat transfer is proportional to  $T^4$ , this represents an increase by almost a factor of two in the heat flux to the roof. This additional heat is of course absorbed by the gasification reaction. The decreased surface temperature when gasification occurs decreases the rate of heat transfer into the coal, but in this case the hot surface remains closer to the steam front due to surface recession. These effects largely compensate each other, such that the total amount of coal heated to the steam temperature is essentially the same for both cases. This simulation, which considered a coal with 20% water content, was ended when the steam flux exiting the reaction front became negative. This occurred at a time of approximately 2.4 h and a penetration depth of the steam front of 6.9 cm.

A value for the group multiplying the diffusion term in equation (17) can now be estimated using representative values  $l = 0.07$  m,  $g = 0.01$  m,  $\dot{l} = 5 \times 10^{-6}$  m s $^{-1}$ ,  $\phi = 0.27$ ,  $T_r = 1100$  K from the numerical solution and an estimate for  $\bar{D}_e$  given by  $\bar{D}_e = \phi^2 \bar{D}_m$ , where  $\bar{D}_m$  is the molecular diffusivity of the

mixture. This semi-theoretical formula for the effective diffusivity in porous solids has been used extensively in the gas-solid reaction literature (see [28]). Estimating  $\bar{D}_m$  to be in the range of  $3 \times 10^{-4}$  m $^2$  s $^{-1}$  gives a value of 0.015 for the dispersion number in equation (17). This is of the order of the activation temperature perturbation parameter  $\delta$ . Inclusion of the dispersion term in the inner-zone equations would result in the leading-order steam balance equation being a function of both  $y_{w0}$  and  $y_{w1}$ , such that a solution could not be obtained. This implies the existence of another boundary layer adjacent to the reactive zone, in which convection of the steam balances diffusion. This dispersion effect is not felt to be of importance in this system, however, since heat transfer controls the supply of steam to the reaction zone, and the heat transfer would not be affected by dispersion. Thus, it is felt adequate for our purposes to allow the matching conditions with the outer zone given by (29).

A number of simulations were performed with different values for the failure parameters  $T_f$  and  $l_f$ . Typically, only one or two spalls were sufficient to reach a quasi-steady state in which the spalling time was constant. The mean roof recession rate  $v_r$  is defined as  $l_f/t_{sp}$ , while the spalling velocity  $v_{sp}$  into the char bed is  $(l_f - g)/t_{sp}$ . Mean values for the recession and spalling velocities, surface temperature and heat transfer over a (constant) spalling time were used to couple energy and material balances between a coal roof and a gasifying char bed, given a flux and composition of a feed gas injected into the bottom of the char bed, to determine conditions for quasi-steady operation of the coupled system for times long compared with the spalling time. That is, conditions in which the rate of carbon from the roof balanced the carbon conversion rate in the bed were sought. Details of this exercise in are described

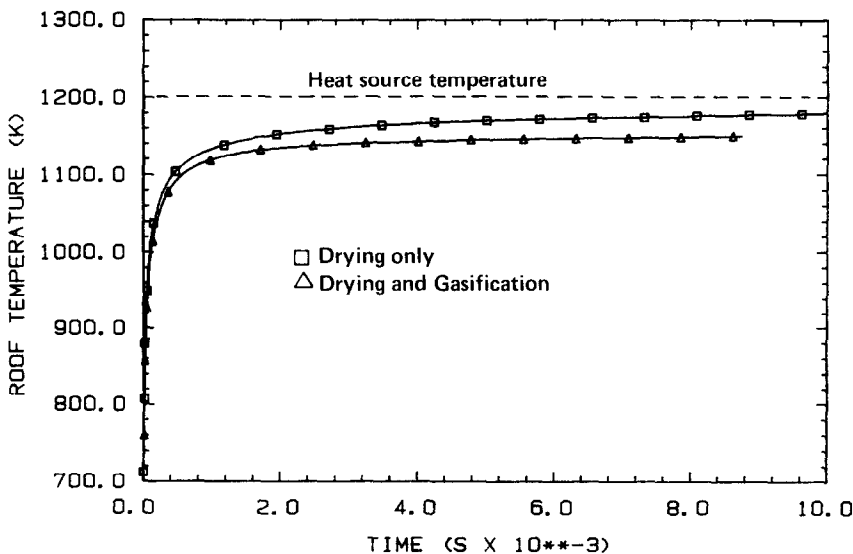


FIG. 6. Comparison of roof surface temperatures as functions of time for drying and drying plus gasification. Latter simulation ended when complete consumption of exiting steam occurred.

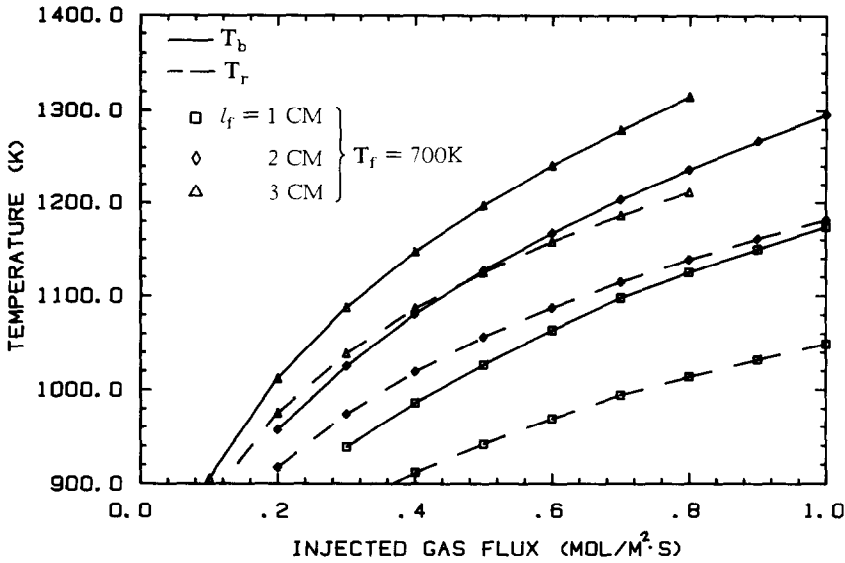


FIG. 7. Char bed and roof surface temperatures as functions of the injected gas flux to the char bed (33%O<sub>2</sub>, 67%H<sub>2</sub>O), for various failure length parameter values.

elsewhere [29]. It was found that while the failure parameters influence the char bed and roof surface temperatures, the overall roof recession rate was quite insensitive to these parameters, and depended largely only on the oxygen flux to the char bed. This is shown in Figs. 7 and 8. An increase in coal strength (increase in  $l_f$  and/or  $T_f$ ) increases the roof surface and char bed temperatures (Fig. 7), with the net effect of increasing heat transfer to the roof. Less conversion in the char bed is evidenced due to the higher heat loss, but more gasification occurs at the roof, such that the overall roof recession rate (gasification plus spalling) remains essentially constant (Fig. 8), decreasing only slightly

due to increased sensible heat loss to the void gas at higher cavity temperatures. Cavity temperatures as high as 1373 K have been recorded in small-scale UCG burns [30] which evidenced spalling behavior [2]. Thus, both roof gasification and spalling appear to play an active role in these UCG systems and their combination by such a mechanism as studied here may offer an explanation for the observation that overall roof recession rates in UCG field tests are relatively constant and insensitive to a number of operating conditions. Another result of this study was that for coals characterized by reasonable values for  $T_f$  and  $l_f$  and of typical moisture content (20%), injected steam

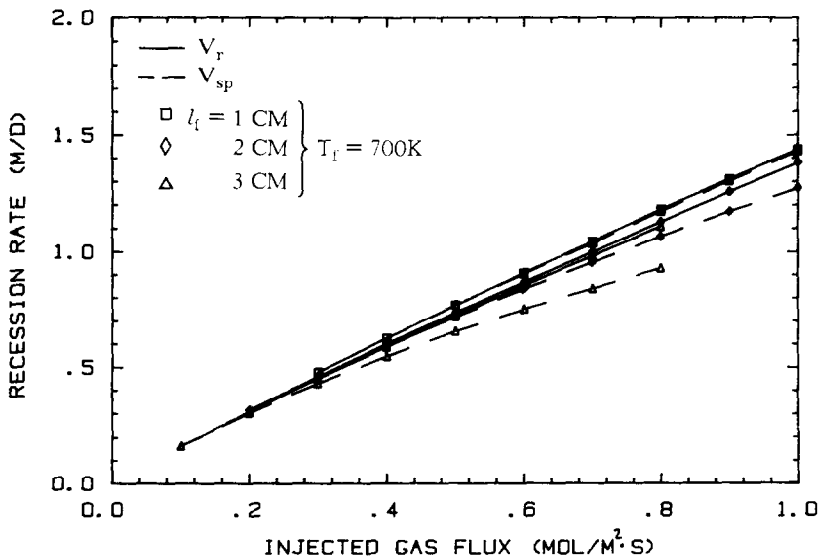


FIG. 8. Total roof and spalling recession rates as functions of the injected gas flux to the char bed, for various failure length parameter values. Conditions of Fig. 7.

acts only as a diluent, and thus the carbon conversion rate for air and for a 21%O<sub>2</sub>-79%H<sub>2</sub>O mix, for example, would be almost identical.

Pyrolysis reactions must be treated numerically in the simulation of the roof dynamics, since, although individual pyrolysis reactions are activated, there are many such reactions evolving different species at different temperatures and locations within the dry coal, and the net result is a distributed release. The net heat effect of the pyrolysis reactions is generally considered to be neutral, such that only countercurrent convection of the released gases need be considered in the energy balance. Pyrolysis was modeled as the evolution of a single pseudo-component released from the solid at a rate first-order in the local amount of volatile matter remaining in the dry coal, according to one-step Arrhenius kinetics, with kinetic constants chosen deliberately low to simulate the distributed process. The pyrolysis data of Campbell [31] show that for a Wyoming sub-bituminous coal gas is evolved over a temperature range of approximately 600–1200 K, with a mean (on a molar basis, including condensible species) of about 800 K. The first peak of the CO pyrolysis trace given in ref. [31] appears appropriate for modeling a single 'effective' pyrolysis reaction. The kinetic constants for this peak were measured to be  $A_p = 55 \text{ s}^{-1}$ ,  $T_{ap} = 9070 \text{ K}$ . The equations describing pyrolysis in the dry coal for the case of no surface reaction ( $g = 0$ ):

$$\frac{\partial W_v}{\partial t^*} = \frac{\eta^i}{l} \frac{\partial W_v}{\partial \eta} - A_p W_v e^{-T_{ap}/T^*} \quad (43)$$

$$F_{sp}(\eta) = \frac{l \rho_s A_p}{M_{sp}} \int_1^\eta W_v e^{-T_{ap}/T^*} d\zeta. \quad (44)$$

were incorporated into the numerical solution, and the energy balance (15) was modified to account for convection of the released gases and the density de-

crease of the solid phase. Upwind differencing of the convective term in (43) was required for numerical stability. The surface temperature as a function of time for drying and drying plus pyrolysis are shown in Fig. 9. In this simulation,  $l_f = 2 \text{ cm}$  and  $T_f = 700 \text{ K}$ , and the total gas flux exiting the coal face was slightly more than twice the amount, on a molar basis, for the case considering pyrolysis. It appears that a longer time is required for steady spalling conditions to evolve when pyrolysis is included, but the latter spalls are very similar for both cases, indicating that the convective cooling effect of the pyrolysis gases is of minor importance. This is certainly true with respect to the heat effect of the gasification. Pyrolysis is more important as a reactant source for gasification, since significant amounts of CO<sub>2</sub> and decomposition water are typically produced at low temperatures relative to the other pyrolysis products. Attempts to extend this model to regimes beyond complete reaction of evaporated water should consider reactive pyrolysis gases as well as diffusion of reactants from the void gas to the solid surface. The former source can be realistically approximated by adding an estimate of the amount of pyrolysis water and CO<sub>2</sub> formed per unit mass of dry coal, at a rate given by the steam front velocity, to the flux of steam entering the reaction zone.

## CONCLUSIONS

A one-dimensional, unsteady-state model has been developed to study effects of drying, pyrolysis, gasification and thermomechanical failure of a coal face exposed to a high temperature. The model equations for unsteady heat penetration into the roof, pyrolysis and spalling are solved numerically, but gasification at the roof surface by steam evaporated from the coal interior is described by a set of equations derived from a simplified singular perturbation solution of the

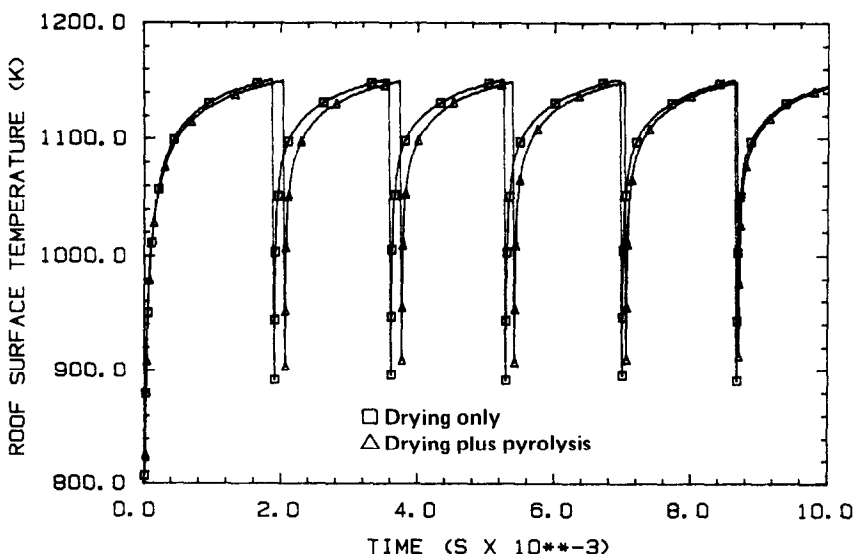


FIG. 9. Comparison of surface temperatures with time for roof drying, and drying plus pyrolysis.

reaction rate equations, based on the large activation energy of the steam/char reaction. This solution is valid for nonplanar surfaces as well, if the radius of curvature of the surface is large compared with the normal thermal penetration distance. Two spalling parameters, an average failure length and a failure temperature, characterize the thermomechanical response of the roof coal.

Radiation dominates as the heat transfer mechanism to the coal face. Pyrolysis was found to have a minor thermal effect on the roof dynamics, although it can be a significant reactant source for gasification. Gasification and spalling can be simultaneously important mechanisms for recession of a coal cavity surface. The failure parameters influence the mechanism for roof recession by altering the relative importance of gasification compared with spalling, but the overall roof recession rate is remarkably insensitive to these parameters, and depends principally on the oxygen flux to the reactive char bed formed by spalling of the roof coal. Thus, consideration of both gasification and thermomechanical failure of the roof coal is necessary to explain the relative insensitivity of vertical cavity growth to operating conditions, observed in a number of UCG field tests.

*Acknowledgements*—Support for this work was provided by Lawrence Livermore National Laboratory under the auspices of the U.S. Department of Energy, contract No. W-7405-ENG-48. Helpful discussions with Dr C. B. Thorsness of LLNL are greatly appreciated.

## REFERENCES

1. A. D. Youngberg and D. J. Sinks, Postburn study results for Hanna II Phases II and III underground coal gasification experiment, *Proc. 7th Underground Coal Conversion Symp.*, LLNL report Conf-810923 8-16 (1981).
2. A. L. Ramirez, D. G. Wilder and G. A. Pawloski, Examination of UCG cavities for the large block test, Centralia, Washington, *Proc. 8th Underground Coal Conversion Symp.*, Sandia National Lab. report SAND82-2355 365-376 (1982).
3. R. E. Glass, The effect of thermal and structural properties on the growth of an underground coal gasification cavity, *Proc. 9th Underground Coal Conversion Symp.*, U.S. DOE report DOE/METC/84-7, 304-313 (1983).
4. H. R. Sutherland, P. J. Hommert, L. M. Taylor and S. E. Benzely, Subsidence prediction for the forthcoming TONO project, *Proc. 9th Underground Coal Conversion Symp.*, U.S. DOE report DOE/METC/84-7, 99-108 (1983).
5. S. H. Advani, O. K. Min, S. M. Chen, J. K. Lee, B. L. Aboustit and S. C. Lee, Stress mediated response associated with UCG cavity and subsidence prediction modeling, *Proc. 9th Underground Coal Conversion Symp.*, U.S. DOE report DOE/METC/84-7, 282-292 (1983).
6. H. R. Mortazavi, A. F. Emery, R. C. Corlett and W. R. Lockwood, The effect of moisture on the structural stability of a coal cavity, presented at 1984 ASME national meeting, New Orleans, LA (1984).
7. J. G. M. Massaquoi, Ph.D. dissertation, West Virginia University, Morgantown, WV (1981).
8. P. A. McMurty, R. C. Corlett, A. F. Emery and H. R. Mortazavi, Comprehensive numerical model of forward combustion along a channel, *Proc. 9th Underground Coal Conversion Symp.*, U.S. DOE report DOE/METC/84-7, 334-339 (1983).
9. A. Liñán, The asymptotic structure of counterflow diffusion flames for large activation energies, *Acta ast.* **1**, 1007-1039 (1974).
10. P. Clavin and F. A. Williams, Effects of molecular diffusion and of thermal expansion on the structure and dynamics of premixed flames in turbulent flows of large scale and low intensity, *J. Fluid Mech.* **116**, 251-282 (1982).
11. N. Peters, Premixed burning in diffusion flames—the flame zone model of Libby and Economos, *Int. J. Heat Mass Transfer* **22**, 691-703 (1979).
12. G. Joulin and P. Clavin, Linear stability analysis of non-adiabatic flames: diffusional-thermal model, *Combust. Flame* **35**, 139-153 (1979).
13. D. R. Kassoy and P. A. Libby, Activation energy asymptotics applied to burning carbon particles, *Combust. Flame* **48**, 287-301 (1982).
14. J. A. Britten and W. B. Krantz, Linear stability of planar reverse combustion in porous media, *Combust. Flame* **60**, 125-140 (1985).
15. J. Buckmaster and G. S. S. Ludford, *Theory of Laminar Flames*. Cambridge University Press, Cambridge (1982).
16. B. Laub, K. E. Suchsland and A. L. Murray, Mathematical modeling of ablation problems, *ASME Appl. Mech. Div.* **30**, 87-115 (1878).
17. M. A. Gibson and C. A. Euker, Mathematical modeling of fluidized bed coal combustion, AICHE Symp. on Laboratory Reactors, Los Angeles, CA (1975).
18. S. Badzoich, D. R. Gregory and M. A. Field, Investigation of the temperature variation of the thermal conductivity and thermal diffusivity of coal, *Fuel* **43**, 267-280 (1964).
19. A. G. Hansen, *Similarity Analyses of Boundary Value Problems in Engineering*. Prentice-Hall, Englewood Cliffs, NJ (1964).
20. R. W. Lyczkowski and Y. T. Chao, Comparison of Stefan model with two-phase model of coal drying, *Int. J. Heat Mass Transfer* **27**, 1157-1169 (1984).
21. J. A. Britten and W. B. Krantz, Linear stability of a planar reverse combustion front propagating through a porous medium: gas-solid combustion model. In *Chemical Instabilities*, edited by G. Nicolis and F. Baras, pp. 117-135. Reidel, Dordrecht (1984).
22. G. Joulin and T. Mitani, Linear stability analysis of two-reactant flames, *Combust. Flame* **40**, 235-246 (1981).
23. R. F. Sincovec and N. K. Madsen, Software for nonlinear partial differential equations, *ACM Trans. Math. Software* **1**, 232-260 (1975).
24. A. C. Hindmarsh, LSODE and LSODI, two new initial value ordinary differential equation solvers, *ACM-Signum News* **4**, 10-11 (1980).
25. A. Amr, Analysis of reverse combustion in tar sands, *Combust. Flame* **41**, 301-312 (1981).
26. F. G. Blottner, Analytical solutions for predicting coal drying, Sandia National Lab. report SAND82-0758, Albuquerque, NM (1982).
27. Mondy, L. A. and F. G. Blottner, The drying of coal in underground coal gasification, *Proc. 8th Underground Coal Conversion Symp.*, Sandia National Lab. report SAND82-2355 355-364 (1982).
28. J. M. Smith, *Chemical Engineering Kinetics*, 3rd edn, pp. 462-468. McGraw-Hill, New York (1981).
29. J. A. Britten and C. B. Thorsness, Modeling thermal and material interactions between a reacting char bed and a gasifying/spalling coal roof, *Proc. 11th Underground Coal Conversion Symp.*, U.S. DOE report DOE/METC-85/6028 365-380 (1986).
30. R. W. Hill and C. B. Thorsness, Summary report on large block experiments in underground coal gasification, Tono Basin, Washington: Vol. 1. *Experimental Description and Data Analysis*. Lawrence Livermore National Lab. report UCRL-53305 Livermore, CA (1982).
31. J. H. Campbell, Pyrolysis of sub-bituminous coal in relation to *in situ* coal gasification, *Fuel* **57**, 217-224 (1978).

## RECESSION D'UNE FACE FROIDE EXPOSEE A UNE TEMPERATURE ELEVEE

**Résumé**—On développe un modèle monodimensionnel variable pour décrire le séchage, la pyrolyse, la gazéification endothermique et la fragmentation (fracture thermomécanique) d'une surface de charbon humide exposée à une température élevée. Une situation semblable apparait, par exemple, au sommet d'une cavité souterraine de gazéification du charbon (UCG). L'intérêt est porté sur la thermochimie et la mécanique des roches qui sont simplifiées par l'utilisation de deux paramètres, une longueur de fracture et la température, qui mesurent la résistance du charbon. Le séchage du charbon et la convection de l'eau évaporée sont modélisés comme dans un problème de Stefan et la réaction de cette vapeur d'eau avec le carbone à la surface libre est décrite par une solution asymptotique dans la limite d'une grande énergie d'activation pur cette réaction. Ainsi les effets de l'évaporation et de la gazéification deviennent des conditions aux limites analytiques pour la solution numérique de la pénétration variable de la chaleur dans le charbon froid. La pyrolyse est traitée numériquement comme l'enlèvement d'un composant unique dans le charbon sec selon une cinétique d'Arrhenius à échelon. La gazéification et la fragmentation sont toutes deux importantes pour les conditions de l'UCG. Le modèle, en particulier la solution de perturbation développée pour la vitesse de récession de la surface due à la gazéification, a des applications dans la pyrolyse ablativ et les systèmes connexes.

## OBERFLÄCHENVERÄNDERUNG BEI EINER UNTER HOHER TEMPERATUR STEHENDEN KOHLEFLÄCHE

**Zusammenfassung**—Es wurde ein eindimensionales transientes Modell entwickelt zur Beschreibung der Vorgänge beim Trocknen, bei der Pyrolyse, der endothermen Vergasung und dem Zersetzen einer nassen Kohleoberfläche bei hoher Temperatur. Solche Vorgänge treten z. B. bei unterirdischen Kohlevergasungsverfahren (UCG) auf. Besondere Aufmerksamkeit gilt den thermochemischen Vorgängen, die gesteinsmechanischen Vorgänge konnten vereinfacht beschrieben werden durch Verwendung zweier Parameter, einer Einrißlänge und Temperatur, welche die Festigkeitseigenschaften der Kohle bestimmen. Der Trocknungsvorgang und die Konvektion des dabei verdampfenden Wassers wird gemäß einem Stefan-Modell dargestellt, und die Reaktion des Wasserdampfes mit Kohlenstoff an der freien Oberfläche wird durch eine asymptotische Lösung im Bereich großer Aktivierungsenergien beschrieben. Dadurch wird erreicht, daß Verdampfungs- und Vergasungseffekte als analytische Randbedingungen mit in die numerische Lösung zur Beschreibung des transienten Wärmedurchgangs in der trockenen Kohle eingehen. Die Pyrolyse wird numerisch dargestellt als Abspaltvorgang einer einzelnen Komponente der trockenen Kohle, gemäß den Grundlagen von Arrhenius. Es zeigte sich, daß sowohl die Oberflächenvergasung als auch die Zersetzung Einfluß auf die typischen UCG-Betriebsbedingungen haben und ihre gegenseitige Abhängigkeit Aufschlüsse für UCG-Testbeobachtungen liefern kann. Das Modell, insbesondere der Störungsansatz für Oberflächenveränderungen infolge Vergasung, kann für pyrolytisch abtragende oder ähnliche Vorgänge angewendet werden.

## ЗАГЛУБЛЕНИЕ ПОВЕРХНОСТИ УГЛЯ ПОД ВОЗДЕЙСТВИЕМ ВЫСОКОЙ ТЕМПЕРАТУРЫ

**Аннотация**—Разработана одномерная переходная модель для описания сушки, пиролиза, эндотермической газификации и растрескивания (термомеханический распад) поверхности влажного угля под воздействием высокой температуры. Такая ситуация возникает, например, на кровле подземной камеры газификации угля (ПКГ). Особое внимание уделяется термохимическому механизму, а уравнения горной механики упрощаются за счет применения двух параметров—длины растрескивания и температуры, которые определяют прочность угля. Сушка угля и конвективный перенос испаряющейся жидкости моделируются как задача Стефана, а реакция водяного пара с углеродом на свободной поверхности описывается асимптотическим решением в пределе большой энергии активации для данной реакции. Таким образом, эффекты испарения и газификации становятся аналитическими условиями при численном решении уравнений для нестационарного распространения тепла в сухом угле. Пиролиз рассматривается численно, как выделение единичного компонента в сухом угле в соответствии с кинетикой Аррениуса. Показано, что как газификация поверхности, так и растрескивание являются важными условиями для типичных ПКГ, а их относительное взаимодействие может служить объяснением наблюдений, полученных при полевых испытаниях. Эта модель, в частности, решена методом возмущений. Полученное соотношение для скорости заглубления поверхности в результате газификации применяется при расчете пиролиза разрушающихся систем.